On strongly correlated electrons in metals

Jacob Szeftel*
ENS Paris-Saclay/LuMIn, 4 avenue des Sciences, 91190 Gif-sur-Yvette, France

A procedure, dedicated to superconductivity, is extended to study the properties of interacting electrons in normal metals in the thermodynamic limit. Each *independent*-electron band is shown to split into two *correlated*-electron bands. Excellent agreement is achieved with Bethe's wave-function for the one-dimensional Hubbard model. The groundstate energy, reckoned for the two-dimensional Hubbard Hamiltonian, is found to be *lower* than values, obtained thanks to the numerical methods. This analysis applies for any spatial dimension and temperature.

PACS numbers: 71.10.Ca, 71.10.Fd

keywords : inter-electron correlation; BCS theory

I. INTRODUCTION

Although the inter-electron interaction in solid matter is dominated by the Coulomb repulsion, the electron motion has been so far discussed within three of quite *different* frameworks :

- in normal metals, the electrons are known from specific heat and magnetic susceptibility measurements to behave like a Fermi gas of *independent* particles[1], despite the *strong* Coulomb force. Besides, due to an efficient screening of the Coulomb potential, the *repulsive* Hubbard Hamiltonian[2] is believed to describe well the electron motion;
- in the wake of Cooper[3] and BCS[4], the electrons are mostly assumed to be coupled through an *attractive* Hubbard Hamiltonian in superconducting metals;
- in magnetic materials[5–7], the electron motion is usually described with help of the *repulsive* Hubbard, t-J and Heisenberg Hamiltonians.

In addition, a huge numerical effort[2,6,8,9] has been devoted to the many-electron groundstate and a few weakly excited states, believed to account for the $T=0$ and low-temperature properties. Nevertheless, such a state of affairs is unsatisfactory in several respects :

- since the Coulomb repulsion is known to remain *unaltered* at any superconducting or magnetic transition, using a *tailored* Hamiltonian for each physical case is *not* vindicated;
- lacking a reliable criterion for the existence of persistent currents, all authors could but cull *arbitrarily* a theoretical signature of superconductivity[3,4,6,8,10–12], in order to characterise the outcome of their calculations. Unfortunately those assumptions have been invalidated by the recent discovery of a thermodynamical prerequisite for superconductivity[13]. Likewise, an *attractive* inter-electron coupling has been shown *not* to be consistent with persistent currents[14], thermal equilibrium[15], the Josephson effect[16] and occurrence of superconductivity[13,17];
- last but not least, if atoms, molecules and normal metals are indeed observed at $T = 0$ in their groundstate, this is *not* the case for superconductors due to a thermodynamical rationale[13]. Similarly, none of the various magnetic states[5] (antiferro-, ferrimagnetism, spin density wave) can even be an *eigenstate*, not to mention the *groundstate*, of any realistic Hamiltonian, describing the motion of correlated electrons, such as the Hubbard, t-J, Heisenberg ones, which is moreover confirmed by small cluster studies[6]. At last, note that, if the ferromagnetic state is indeed an eigenstate, it is *never* the groundstate in case of an exchange integral $J > 0$.

Therefore, this work is aimed at devising a *single* model, accounting for the $T \geq 0$ properties of normal and superconducting metals, as well. To that end, advantage will be taken of a previous result[18], in order to extend a scheme, developed recently for superconductors[15], to normal metals.

Here is the outline : the concept of the *correlated* Fermi gas will be introduced in the following section to account for the motion of interacting electrons in normal metals at $T = 0$, which will enable us to work out the corresponding correlation functions in the third section; thermal properties at $T > 0$ will be analysed in the fourth section; at last the main results are summarised in the conclusion.

II. CORRELATED FERMI GAS

Let us consider a $d = 1, 2, 3$ dimensional crystal, containing N sites and $2n$ itinerant electrons with $N >> 1, n >> 1$. These electrons of spin $\sigma = \pm 1/2$ populate a single band, accomodating at most two electrons per site ($\Rightarrow n \leq N$). The independent electron motion is

Preprints (www.preprints.org) | NOT PEER-REVIEWED | Posted: 24 December 2021 doi:10.20944/preprints202112.0409.v1

described, in momentum space, by the Hamiltonian H_d

$$H_d = \sum_{k,\sigma} \epsilon(k) c^+_{k,\sigma} c_{k,\sigma} \quad ,$$

for which $\epsilon(k), k$ are the one-electron, spin-independent energy ($\Rightarrow \epsilon(k) = \epsilon(-k)$) and a vector of the Brillouin zone, respectively, and the sum with respect to k is to be carried out over the whole Brillouin zone. Then $c^+_{k,\sigma}, c_{k,\sigma}$ are one-electron creation and annihilation operators on the Bloch[1] state $|k,\sigma\rangle$

$$|k,\sigma\rangle = c^+_{k,\sigma} |0\rangle \quad , \quad |0\rangle = c_{k,\sigma} |k,\sigma\rangle \quad , \qquad (1)$$

with $|0\rangle$ being the no electron state. They enable us to introduce the pair creation and annihilation operators[15,18–21]

$$\begin{array}{lll} b^+_{s,K,k} = c^+_{k,+} c^+_{K-k,-} & , & b_{s,K,k} = c_{K-k,-} c_{k,+} \\ b^+_{t,K,k} = c^+_{k,\sigma} c^+_{K-k,\sigma} & , & b_{t,K,k} = c_{K-k,\sigma} c_{k,\sigma} \end{array} \quad ,$$

with the subscripts s,t referring to *singlet* and *triplet*, because the spin ζ of the corresponding electron pair, projected onto any axis, is equal to $0, \pm 1$, respectively. The hereabove definitions deserve some further comments :

- those pair operators are neither bosons, nor fermions, but their algebraic properties play no role in the following;
- the notation s,t, albeit convenient, is not exact, because the true singlet and triplet pair states with $\zeta = 0$, read actually $\left(b^+_{s,K,k} \pm b^+_{s,K,K-k}\right)|0\rangle$;
- by contrast with singlet pairs for which there is $b^+_{s,K,k} \neq b^+_{s,K,K-k} \Rightarrow \sum_k = N$, triplet pairs are such that $b^+_{t,K,k} = -b^+_{t,K,K-k}$, which entails $\sum_k = \frac{N}{2}$.

Let us introduce now the Hamiltonians H^ζ_K

$$H^\zeta_K = \sum_{k,k'} V^\zeta_{K,k,k'} b^+_{\zeta,K,k} b_{\zeta,K,k'} \quad ,$$

where the matrix element $V^\zeta_{K,k,k'}$ defines the inter-electron interaction. Likewise, the general Hamiltonian, governing the motion of electrons interacting through a two-body force on lattice sites, reads finally

$$H = H_d + \sum_{\zeta,K} H^\zeta_K \quad , \quad \zeta = t,s \quad . \qquad (2)$$

The particular case of the Hubbard Hamiltonian is then characterised by $V^s_{K,k,k'} = U$, $V^t_{K,k,k'} = 0$, $\forall K,k,k'$. H operates[19] inside the Hilbert space S, subtended by a basis of Slater determinants, comprising $2n$ of Bloch states, whereas $H_d + H^\zeta_K$ operates within $S^\zeta_K \subset S$, any vector of the basis of which reads $\prod_{i=1,..n} b^+_{\zeta,K,k_i} |0\rangle$. By contrast, $S_2 \subset S$ is characterised by the property that *none* of its vectors can be written as $\prod_{i=1,..n} b^+_{\zeta,K,k_i} |0\rangle$. Hence, it ensues[19] finally that S, S_2, S^ζ_K are related by

$$S = S_t \oplus S_s \oplus S_2 \quad , \quad S_t = \oplus_K S^t_K \quad , \quad S_s = \oplus_K S^s_K \quad .$$

The BCS scheme[4] was aimed at approximating the many bound electron (*MBE*) eigenstate[15] $\psi^s_{K=0}$ of $H_d + H^s_0$ which is not a realistic Hamiltonian, because it involves four-electron forces, whenever it is Fourier transformed back into real space. Thus ψ^s_K is seen to be of little significance, unless it happens to be an eigenstate of H too. However, due to $\left[H^\zeta_K, H^{\zeta'}_{K'}\right] \neq 0$, this occurs[19] only in the $n = 1$ case, corresponding to a *single* pair[3,15,17]. Nevertheless, by embedding S into a larger Hilbert space, it has been shown[19] that the eigenspectra of $H, H_d + H^s_K$ share indeed common eigenvalues. Hence the significance of this result will be enhanced by the following theorem, the proof of which is given in appendix :
To each eigensolution $\psi^\zeta_K \in S^\zeta_K, \varepsilon$, *fulfilling* $(H_d + H_{K,\zeta} - \varepsilon)\psi^\zeta_K = 0$, *there corresponds, within the thermodynamic limit* $N \to \infty$, *an eigensolution* $\psi \in S, \varepsilon$ *of* H, *such that* $(H - \varepsilon)\psi = 0$ *with* $\psi = \psi^\zeta_K + \phi^\zeta_K$ *and* $\phi^\zeta_K \in S_2$.

This theorem means that a large part of the eigenspectrum of H can be achieved by diagonalising $H_d + H^\zeta_K$, which is much easier[20,21]. Though the eigenvectors $\in S_2$ cannot be obtained in that way[19], this is unimportant, because they are highly *excited* states and thence do *not* give rise to *observable* effects. Besides, the eigenspectrum of $H_d + H^s_K$ consists in a *continuum*[18–21] of many-electron scattering states and a *single MBE* state, responsible for superconductivity[15,17]. A repulsive interaction ($\Rightarrow U > 0$ in case of the Hubbard Hamiltonian) being required for superconductivity to arise[17] entails that the corresponding *MBE* state turns out to be an *excited* state, which confirms a conclusion drawn independently[13] that the superconducting state is *not* the groundstate. As a matter of fact, the $U > 0$ groundstate energy will turn out below to be the lower bound of the *continuum*[18]. Moreover, because the BCS variational scheme[4] has been proved inconsistent due to the $U < 0$ assumption[17], an overhauled version[15,17] will be used below. Since this work is mainly intended at applying the latter to study the *continuum* states, it is in order to recall its tenet. Thus the energy ε of the *MBE* state $\Phi \in S^\zeta_K$ of the Hubbard Hamiltonian is given[15] by

$$\begin{array}{c} \varepsilon = \langle\Phi| \frac{H_d + H^s_K}{N} |\Phi\rangle = \sum_k \varepsilon(K,k) \frac{n^s_{K,k}}{N} + U\Delta^2 \\ \varepsilon(K,k) = \epsilon(k) + \epsilon(K-k) \\ n^s_{K,k} = \langle\Phi| b^+_{s,K,k} b_{s,K,k} |\Phi\rangle \\ \Delta = \sum_k \frac{\sqrt{n^s_{K,k}\left(1 - n^s_{K,k}\right)}}{N} \end{array} \quad . \qquad (3)$$

Minimising[15] ε with $n = \sum_k n^s_{K,k}$ kept constant yields the $\Delta \neq 0$ solution of Eqs.(3) and thence ε.

But the focus will rather be laid below upon the $\Delta = 0$ solutions of Eqs.(3), which implies $n^s_{K,k} = 0$ or $1, \forall K,k$. Thus the corresponding many electron states $\Phi \in S_t \oplus S_s$

Preprints (www.preprints.org) | NOT PEER-REVIEWED | Posted: 24 December 2021 doi:10.20944/preprints202112.0409.v1

are characterised by the following properties, valid for any Hamiltonian H, defined by Eq.(2)

$$\begin{array}{l}\Phi=\varphi_t+\varphi_s \quad , \quad \varphi_t\in S_t \quad , \quad \varphi_s\in S_s \\ \langle\Phi|\, b^+_{\alpha,K,k}b_{\alpha,K,k'}\,|\Phi\rangle=0, \quad \forall K,k\neq k', \quad \alpha=s,t \\ n^\alpha_{K,k}=\langle\Phi|\, b^+_{\alpha,K,k}b_{\alpha,K,k}\,|\Phi\rangle=\langle\varphi_\alpha|\, b^+_{\alpha,K,k}b_{\alpha,K,k}\,|\varphi_\alpha\rangle \Rightarrow . \\ \left\{\begin{array}{l}\sum_{K,k}n^s_{K,k}=\sum_{k,k'}\langle\varphi_s|\, c^+_{k,+}c_{k,+}c^+_{k',-}c_{k',-}\,|\varphi_s\rangle \\ \sum_{K,k}n^t_{K,k}=\sum_{k,k'}\langle\varphi_t|\, c^+_{k,\sigma}c_{k,\sigma}c^+_{k',\sigma}c_{k',\sigma}\,|\varphi_t\rangle\end{array}\right.\end{array}$$

The energy $\varepsilon(\Phi)=\frac{\langle\Phi|H|\Phi\rangle}{N}=\varepsilon_t+\varepsilon_s$ is then inferred to read as a sum of k-dependent, *one-electron* energies, reading for the Hubbard Hamiltonian

$$\begin{array}{l}\varepsilon_t=\langle\varphi_t|\,\frac{H_d}{N}\,|\varphi_t\rangle=\sum_{k,\sigma}\frac{\epsilon(k)}{N}\langle\varphi_t|\, c^+_{k,\sigma}c_{k,\sigma}\,|\varphi_t\rangle \\ \quad=\sum_k\frac{\epsilon_t(k)}{N} \quad , \quad \epsilon_t(k)=\epsilon(k) \\ \varepsilon_s=\sum_{k,\sigma}\frac{\epsilon(k)}{N}\langle\varphi_s|\, c^+_{k,\sigma}c_{k,\sigma}\,|\varphi_s\rangle \\ \quad+\frac{U}{N^2}\sum_{k,k'}\langle\varphi_s|\, c^+_{k,+}c_{k,+}c^+_{k',-}c_{k',-}\,|\varphi_s\rangle \\ \quad=\sum_k\frac{\epsilon_s(k)}{N} \quad , \quad \epsilon_s(k)=\epsilon(k)+U\frac{c_s}{2}\end{array} \quad , \quad (4)$$

where the sum with respect to k is performed over the occupied one-electron states, such that $n_{k,\sigma}=\langle\varphi_{\alpha=t,s}|\, c^+_{k,\sigma}c_{k,\sigma}\,|\varphi_\alpha\rangle=1$. Hence the concentrations $c_t, c_s=c_{s,+}+c_{s,-}$ of *triplet, singlet* electrons are inferred to read

$$\begin{array}{l}c_t=\sum_{k,\sigma}\frac{\langle\varphi_t|c^+_{k,\sigma}c_{k,\sigma}|\varphi_t\rangle}{N} \\ c_{s,+}=\sum_k\frac{\langle\varphi_s|c^+_{k,+}c_{k,+}|\varphi_s\rangle}{N}=\frac{c_s}{2} \\ c_{s,-}=\sum_k\frac{\langle\varphi_s|c^+_{k,-}c_{k,-}|\varphi_s\rangle}{N}=\frac{c_s}{2}\end{array} \quad .$$

The dispersion relations $\epsilon_t(k),\epsilon_s(k)$ in Eqs.(4) characterise every *scattering* state of the continuum. They are typical of a Fermi gas[1], made up of independent electrons, populating *two* one-electron bands. In particular, the groundstate energy $\varepsilon_g=\varepsilon_t+\varepsilon_s$, associated with the lower bound of the continuum, and the corresponding electron concentration $c_0=c_t+c_s$ read

$$\begin{array}{l}c_t=\int_{\epsilon_d}^{E_F}\rho(\epsilon)d\epsilon \quad , \quad \varepsilon_t=\int_{\epsilon_d}^{E_F}\epsilon\rho(\epsilon)d\epsilon \\ c_s=\int_{\epsilon_d}^{e_F}\rho(\epsilon)d\epsilon \quad , \quad \varepsilon_s=\int_{\epsilon_d}^{e_F}\epsilon\rho(\epsilon)d\epsilon+U\frac{c_s^2}{2}\end{array} \quad , \quad (5)$$

with $e_F=E_F-U\frac{c_s}{2}$ and $E_F,\epsilon_d,\rho(\epsilon)$ standing for the Fermi energy, the bottom of the one-electron band of dispersion $\epsilon(k)$ and the corresponding density of states. Likewise $c_t+c_s=c_0\leq 2$ electrons per site entails

$$\int_{\epsilon_d}^{\epsilon_u}\rho(\epsilon)d\epsilon=1 \quad ,$$

with ϵ_u refers to the top of the one-electron band (there is $\epsilon_u=-\epsilon_d$ for the $d=1,2,3$ Hubbard model). It means that each band of dispersion $\epsilon_t(k),\epsilon_s(k)$ can accomodate at most *one* electron, in accordance with the band of dispersion $\epsilon(k)$ accomodating *two* electrons. Noteworthy is that each *independent*-electron band $\epsilon(k)$ is seen to split into two *correlated*-electron bands $\epsilon_t(k),\epsilon_s(k)$, the dispersion of which *depends* upon c_0, unlike $\epsilon(k)$. The identity

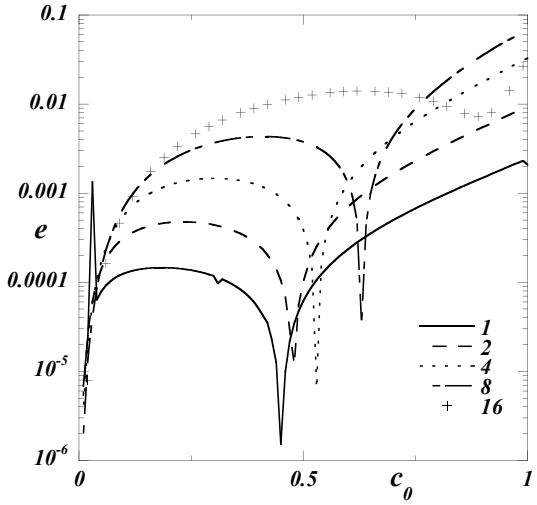

FIG. 1. Semi-logarithmic plot of $e(c_0\leq 1)=\left|\frac{\varepsilon_g(c_0)}{\eta_g(c_0)}-1\right|$; $\varepsilon_g<0,\eta_g<0$ have been obtained by solving Eqs.(6) and with help of Bethe's wave-function, respectively; each curve is labelled by the corresponding U/t value.

$\epsilon_t(k)=\epsilon(k)$ in Eqs.(4,5) is a peculiarity of the Hubbard Hamiltonian, because $\epsilon_t(k)$ would depend explicitly on c_t, as $\epsilon_s(k)$ does on c_s, if two electrons, sitting on neighbouring sites, were allowed to interact, due to $V^t_{K,k,k}\neq 0$. Though the inter-electron coupling is spin-independent, the *two-particle* scattering differs according to whether the two incoming electrons have *same* or *opposite* spins because of $V^t_{K,k,k'}\neq V^s_{K,k,k'}$.

It must be noticed that both *triplet, singlet* bands turn out to be *effective* bands, accounting for the motion of *interacting* electrons, and thence *cannot* be observed in (inverse) photoemission experiments. Likewise they are *unrelated* to the outcome of the *one-electron* band structure calculation.

The groundstate energies $\varepsilon_g(c_0),\eta_g(c_0)$ of the $d=1$ Hubbard model ($\epsilon(k)=-2t\cos(k)$), resulting respectively from Eqs.(5) and Bethe's wave-function[22], are compared in Fig.1. It is more convenient to solve Eqs.(5) in $d=1$ momentum space

$$\begin{array}{l}E_F=\epsilon(k_t)=\epsilon(k_s)+U\frac{c_s}{2} \\ c_t=\frac{k_t}{\pi}, \quad c_s=\frac{k_s}{\pi}, \quad c_0=c_t+c_s \\ \varepsilon_t=-\frac{2t}{\pi}\sin(k_t), \quad \varepsilon_s=-\frac{2t}{\pi}\sin(k_s)+U\frac{c_s^2}{2} \\ \varepsilon_g=\varepsilon_t+\varepsilon_s\end{array} \quad , \quad (6)$$

with $0<k_{\alpha=t,s}<\pi$, $-2t<E_F<2t$. There is perfect agreement $\varepsilon_g=\eta_g=-\frac{2t}{\pi}\sin(\pi c_0)$ for $\frac{U}{t}\to\infty$. This property stems from $c_s(U\to\infty)\to 0,\forall c_0\leq 1$, which entails that all electrons populate the *triplet* band with the *singlet* one remaining empty. Likewise, both Bethe's wave-function[23] and Eqs.(6) yield ε_g and η_g vanishing like $1/U$ for $\frac{U}{t}\to\infty$ and $c_0=1$. The small discrepancy $e(c_0)<<1$, seen in Fig.1 for finite $\frac{U}{t}$, results from the Hilbert space, which Bethe's wave-functions belong in, being different from $S_t\oplus S_s$, because the k_i,k numbers,

Preprints (www.preprints.org) | NOT PEER-REVIEWED | Posted: 24 December 2021 doi:10.20944/preprints202112.0409.v1

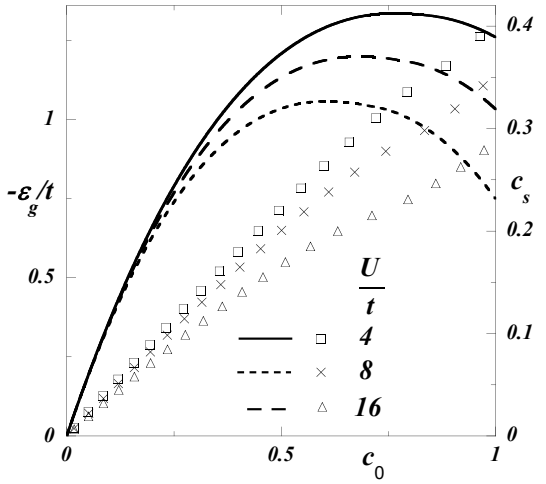

FIG. 2. Plots of $\varepsilon_g(c_0) < 0$ as solid, dashed and dotted lines and $c_s(c_0)$ as squares, $\times$ and triangles, obtained by solving Eqs.(7) for $U/t = 4, 8, 16$, respectively; the scale for ε_g, c_s is on the left and right side, respectively.

subtending respectively Bethe's wave-functions and the Bloch-like basis $\{|k,\sigma\rangle\}$, defined in Eq.(1), obey *different* periodic boundary conditions.

Though Bethe's wave-function is an *eigenstate* of H, whereas Φ_g, solution of Eqs.(5,6), is *not*, both share the same significance, insofar as the energy of *interacting* electrons is found as a sum over the energies of *independent* particles, but with a density of states *renormalised* by U, c_0, as illustrated by $\rho(\epsilon) + \rho(\epsilon - U\frac{c_s}{2})$ showing up instead of $2\rho(\epsilon)$ for the $U = 0$ case. But by contrast with Bethe's wave-function, Eqs.(5) *apply* for $d > 1, T > 0$, as seen below. Noteworthy is that none of the numerous numerical approximations[8,24] has achieved the remarkable agreement, displayed in Fig.1.

Values of $\varepsilon_g(E_F) = \varepsilon_t(E_F) + \varepsilon_s(E_F)$ have also been obtained for the $d = 2$ Hubbard model and plotted in Fig.2. It is more convenient to solve Eqs.(5) in $d = 2$ momentum space

$$\begin{array}{l} c_{\alpha=t,s} = \int\int_{\Omega_\alpha} \frac{dk_x dk_y}{\pi^2} \Rightarrow c_0 = c_t + c_s \\ \varepsilon_t = \int\int_{\Omega_t} \epsilon\,(k_x,k_y)\,\frac{dk_x dk_y}{\pi^2} \\ \varepsilon_s = \int\int_{\Omega_s} \epsilon\,(k_x,k_y)\,\frac{dk_x dk_y}{\pi^2} + U\frac{c_s^2}{2} \\ \varepsilon_g = \varepsilon_t + \varepsilon_s \end{array} \quad , \qquad (7)$$

with $\epsilon\,(k_x,k_y) = -2t\,(\cos(k_x) + \cos(k_y))$, $0 < k_{x,y} < \pi$, $-4t < E_F < 4t$ and the respective integration domains Ω_t, Ω_s being defined by $\epsilon\,(k_x,k_y) < E_F$, $\epsilon\,(k_x,k_y) < e_F$. Those data have been compared in table I with the corresponding values, obtained by means of an exact diagonalisation, performed in a $N = 16$ cluster[25]. There is $\varepsilon_g < \eta_g$ and the discrepancy is seen to increase with growing n_e. A similar discrepancy is seen in table II, illustrating a comparison between this work and the numerical methods[8], applied to the $d = 2$ Hubbard Hamiltonian. The latter is likely to result from a common shortcoming of all numerical procedures, since the groundstate

TABLE I. Comparison of $\varepsilon_g < 0$ inferred from Eqs.(7) with $\eta_g < 0$ resulting from the diagonalisation[25] of a $N = 16$ cluster; values of ε_g/η_g are listed for various $n_e, U/t$ with n_e being the number of electrons ($c_0 = n_e/N$).

n_e	c_0	$\frac{U}{t}=20$	$\frac{U}{t}=10$	$\frac{U}{t}=8$	$\frac{U}{t}=4$
16	1	2.79	2.15	1.95	1.48
15	.938	2.03	1.84	1.73	1.42
14	.875	1.63	1.6	1.55	1.34
13	.813	1.42	1.44	1.41	1.27
12	.75	1.26	1.29	1.28	1.21
11	.688	1.15	1.19	1.18	1.14
10	.625	1.05	1.09	1.09	1.04
9	.562	1.05	1.1	1.1	1.09
8	.5	1.04	1.09	1.1	1.1
7	.438	1.05	1.1	1.1	1.1

energy is extrapolated from a small value $N < 100$ up to $N \to \infty$. Because the dimension of the Hilbert space grows exponentially with N, there is *no* one to one correspondence between the eigenspectra associated with $N, N+1$, so that it is impossible to ensure that the procedure is indeed converged toward the groundstate for $N \to \infty$. Accordingly, the data in table I, obtained for $c_0 = 1, .875$ and $\frac{U}{t} = 4, 8$, are seen to be close to corresponding values in table II, which hints further at the extrapolation schemes[8] missing the groundstate for $N \to \infty$.

Our interest in the $\Delta = 0$ solution of Eqs.(3) arose from solving the Schrödinger equation for one singlet pair, which reads for the one-dimensional Hubbard Hamiltonian[15,17]

$$\begin{array}{c} (H_d + H_K^s - \varepsilon)\,\psi = 0, \quad \psi = \sum_k a(k) b^+_{s,K,k}\,|0\rangle \\ a(k)\,(\varepsilon - \varepsilon(K,k)) = \delta = \sum_k a(k) \\ \frac{1}{U} = \frac{1}{N}\sum_k \frac{1}{\varepsilon - \varepsilon(K,k)} \end{array} \quad . \qquad (8)$$

If $\pm t_K$ are the maximum and minimum of $\varepsilon(K,k)$ over k, Eqs.(8) have one solution $\varepsilon = \varepsilon_B > t_K$ ($< -t_K$) for $U > 0$ ($U < 0$), associated with the single bound pair, characterised by $\delta \neq 0$ and $(N-1)$ solutions $\varepsilon_{i=1,\ldots N-1} \in [\varepsilon(K,k_i), \varepsilon(K,k_{i+1})]$ with $\varepsilon(K,k_1) = -t_K, \varepsilon(K,k_N) = t_K, k_{i+1} - k_i = \frac{2\pi}{N}$. Then $N \to \infty$ implies $(k_{i+1} - k_i) \to 0 \Rightarrow \varepsilon_i \to \varepsilon(K,k_i) \Rightarrow \delta \to 0$. Thus the ε_i's, making up the continuum $[-t_K, t_K]$ in the $N \to \infty$ limit ($\Rightarrow \delta = 0$), and the $\delta \neq 0$ solution of Eqs.(8) are realized to turn into the $\Delta = 0, \Delta \neq 0$ solutions of Eqs.(3), associated with the scattering and bound states at *finite* c_0, respectively.

Replacing electrons by holes yields the following relation[22]

$$\varepsilon(c_0) = \varepsilon(2 - c_0) + U(c_0 - 1) \quad . \qquad (9)$$

Then derivating Eq.(9) with respect to c_0 for half-filling $c_0 = 1$, while keeping in mind that $\frac{\partial \varepsilon_g}{\partial c_0} = E_F$ at $T = 0$,

Preprints (www.preprints.org) | NOT PEER-REVIEWED | Posted: 24 December 2021 doi:10.20944/preprints202112.0409.v1

TABLE II. Comparison of $\varepsilon_g < 0$ inferred from Eqs.(7) with $\eta_g < 0$, the average data resulting from the numerical procedures[8] at $T = 0$; values of ε_g/η_g are listed for various $c_0, U/t$.

c_0	$\frac{U}{t}=2$	$\frac{U}{t}=4$	$\frac{U}{t}=6$	$\frac{U}{t}=8$	$\frac{U}{t}=12$
1	1.21	1.47	1.73	1.98	2.38
.875	1.13	1.29	1.45	1.58	
.8	1.11	1.21	1.32	1.39	

because free energy and energy are thence equal[26], leads to

$$E_F(1^-) + E_F(1^+) = U \Rightarrow E_g = U - 2E_F(1^-) \quad ,$$

wherein E_g is a forbidden gap of the one-electron band structure[22]. Hence Eqs.(5) are inferred to be valid for $c_0 \leq 1$ for $U > 0$. Such a result seems to run afoul at alcali and noble metals being good conductors in spite of their half-filled s conduction band ($\Rightarrow c_0 = 1$). Actually the $s-p$ hybridisation is likely to be responsible for no E_g-like gap opening up in the middle of their conduction band. Moreover the significance of this explanation is further strengthened by earth-alcali metals, since, in the absence of hybridisation, they should be insulators due to $c_0 = 2$.

III. TWO-BODY CORRELATION PROPERTIES

The correlation properties of the correlated Fermi gas will be exemplified on antiferromagnetic compounds, such as NiO, MnO, CoO, which should behave like metals[7], if the electrons were independent, because the conduction band is half-filled ($\Leftrightarrow c_0 = 1$). Such a property was argued[31,32] to ensue from a large Hubbard repulsion ($\Leftrightarrow U/t >> 1$ with t characterising the one-electron bandwidth and thence average kinetic energy). Conversely the correlated Fermi gas will be shown below to sustain no antiferromagnetic order $\forall U > 0, c_0 \leq 1$.

The long-range antiferromagnetic order is characterised by the parameter

$$\Delta_{AF}(|r|) = \sum_{i,j} \langle \Phi \left| c^+_{i,+} c_{i,+} c^+_{j,-} c_{j,-} \right| \Phi \rangle \quad ,$$

where Φ stands for the considered many-electron state, r_i, r_j are position vectors, pertaining to sites i, j ($r = r_i - r_j$) and $c^+_{i,\sigma}, c_{i,\sigma}$ are one-electron creation and annihilation operators on the Wannier[1] state $|i,\sigma\rangle$

$$|i,\sigma\rangle = c^+_{i,\sigma} |0\rangle \quad , \quad |0\rangle = c_{i,\sigma} |i,\sigma\rangle \quad .$$

Then Φ is said to have long range order, provided Δ_{AF} is a periodic function of $|r|$ for $|r| \to \infty$ with the period equal to twice the lattice parameter. Actually Δ_{AF} reads for every Φ, obeying Eqs.4

$$\Delta_{AF} = \sum_{k,k'} \frac{\cos\left((k-k').r\right)}{N} \left\langle \varphi_s \left| c^+_{k,+} c_{k,+} c^+_{k',-} c_{k',-} \right| \varphi_s \right\rangle ,$$

where the sum is to be carried out on occupied *singlet* electrons, only, because there is $\Delta_{AF} = 0, \forall |r|$ for *triplet* electrons. For the $d = 1$ groundstate defined by Eqs.6, Δ_{AF} reads

$$\Delta_{AF} = |r|^{-2} \quad ,$$

which implies $\Delta_{AF}(r) \to 0$ for $|r| \to \infty$. Since that conclusion holds also for $d > 1$, any kind of two-electron correlation and every Φ, obeying Eqs.4, the correlated Fermi gas is inferred to sustain no long-range order whatsoever, like the Fermi gas of independent particles[1]. Besides, there is even $\Delta_{AF} = 0, \forall |r|$ for $U \to \infty$ due to $c_s \to 0$. The conclusion, that the Hubbard model with $c_0 < 1$ remains metallic even for $U \to \infty$, had been drawn previously[22], but for $d = 1$. This work shows that it is true for $d > 1$, too.

By contrast, the numerical methods[2,6,8,9] yield, in the $d = 2$ case, various ordered structures, such as stripes, spin or charge density waves for $c_0 \approx 1$, which are *not* observed. This reinforces the argument, presented in the preceding section, that the outcome of such numerical procedures is to be associated with an excited state, possibly belonging in S_2, because any scattering state $\Phi \in S_t \oplus S_s$ has been shown above to display no long range order. Likewise, the small cluster calculations[6] conclude on the $d = 2$ Hubbard model sustaining no magnetic order, whereas the numerical approximations[8] come to the opposite conclusion, though both lead to groundstate energies close to one another, as already mentioned above.

For the sake of illustration, we give the probability of double occupancy o_2, reading for the groundstate Φ_g with $d = 1, 2, 3$ as

$$\begin{aligned} o_2 &= \textstyle\sum_i \left\langle \Phi_g \left| \frac{c^+_{i,+} c_{i,+} c^+_{i,-} c_{i,-}}{N} \right| \Phi_g \right\rangle \\ &= \textstyle\sum_{k,k'} \left\langle \varphi_s \left| \frac{c^+_{k,+} c_{k,+} c^+_{k',-} c_{k',-}}{N^2} \right| \varphi_s \right\rangle = \left(\frac{c_s}{2}\right)^2 \end{aligned} \quad .$$

As seen in table III, there is always $o_2 < p_2$ with p_2 reckoned with help of the numerical procedures[8]. Such an inequality is in keeping with $\varepsilon_g < \eta_g$ in table II, because the correlated Fermi gas manages to lower its energy by accomodating as many electrons as possible in the *triplet* band, for which double occupancy is forbidden by Pauli's principle.

Preprints (www.preprints.org) | NOT PEER-REVIEWED | Posted: 24 December 2021 doi:10.20944/preprints202112.0409.v1

TABLE III. comparison of double occupancy o_2 inferred from Eqs.(7) with p_2, the average data resulting from the numerical procedures[8] at $T = 0$; values of p_2/o_2 are listed for $c_0 = 1$ and various U/t.

$\frac{U}{t} = 2$	$\frac{U}{t} = 4$	$\frac{U}{t} = 6$	$\frac{U}{t} = 8$	$\frac{U}{t} = 12$
3.96	3.15	2.29	1.74	1.11

IV. THERMAL PROPERTIES

For $T > 0, c_0 \leq 1$, Eqs.(5) are recast into

$$\begin{array}{c} c_t = \int_{\epsilon_d}^{\epsilon_u} \rho(\epsilon) n(\epsilon) d\epsilon \quad , \quad \varepsilon_t = \int_{\epsilon_d}^{\epsilon_u} \epsilon \rho(\epsilon) n(\epsilon) d\epsilon \\ c_s = \int_{\epsilon_d}^{\eta_u} \rho(\epsilon) n(\epsilon + U\frac{c_s}{2}) d\epsilon \\ \varepsilon_s = \int_{\epsilon_d}^{\eta_u} \epsilon \rho(\epsilon) n(\epsilon + U\frac{c_s}{2}) d\epsilon + U\frac{c_s^2}{2} \end{array} , \quad (10)$$

with $\eta_u = \epsilon_u - U\frac{c_s}{2}$ and $n(\epsilon) = \left(1 + e^{\frac{\epsilon - E_F}{k_B T}}\right)^{-1}$ standing for the Fermi-Dirac distribution[1] (k_B designates Boltzmann's constant). The specific heat $C(T) = \frac{d\varepsilon_t}{dT} + \frac{d\varepsilon_s}{dT}$ can be reckoned thanks to Eqs.(10) as follows

$$\begin{array}{l} \frac{d\varepsilon_t}{dT} = -\int_{\epsilon_d}^{\epsilon_u} \epsilon \rho(\epsilon) \left(\frac{dE_F}{dT} + \frac{\epsilon - E_F}{T}\right) \frac{\partial n}{\partial \epsilon}(\epsilon) d\epsilon \\ \frac{d\varepsilon_s}{dT} = \int_{\epsilon_d}^{\eta_u} \epsilon \rho(\epsilon) \left(\frac{U}{2}\frac{dc_s}{dT} - \frac{dE_F}{dT} - \frac{\epsilon - e_F}{T}\right) \frac{\partial n}{\partial \epsilon}(\epsilon + U\frac{c_s}{2}) d\epsilon \\ \quad + U c_s \frac{dc_s}{dT} \end{array} .$$

Since the correlated electrons make up a degenerate Fermi gas ($\Rightarrow T << E_F/k_B$), the Sommerfeld expansion[1] can be applied, which yields at T^2 order

$$\begin{array}{c} \frac{dc_t}{dT} = \frac{dE_F}{dT} a(E_F) + \frac{(\pi k_B)^2}{3} \frac{d\rho}{d\epsilon}(E_F) T \\ \frac{dc_s}{dT} = \frac{\frac{dE_F}{dT} a(e_F) + \frac{(\pi k_B)^2}{3} \frac{d\rho}{d\epsilon}(e_F) T}{1 + \frac{U}{2} a(e_F)} \end{array} ,$$

with $a(\epsilon) = \rho(\epsilon) + \frac{(\pi k_B T)^2}{6} \frac{d^2\rho}{d\epsilon^2}(\epsilon)$. Then taking advantage of $c_t(T) + c_s(T) = c_0 \Rightarrow \frac{dc_t}{dT} + \frac{dc_s}{dT} = 0$ yields finally

$$\begin{array}{l} \frac{dE_F}{dT} = -\frac{(\pi k_B)^2 \left(\frac{d\rho}{d\epsilon}(e_F) + \frac{d\rho}{d\epsilon}(E_F)\left(1 + \frac{U}{2}a(e_F)\right)\right)}{3\left(a(e_F) + a(E_F)\left(1 + \frac{U}{2}a(e_F)\right)\right)} T \Rightarrow \\ C = \left(\frac{dE_F}{dT} - \frac{U}{2}\frac{dc_s}{dT}\right) f_2(e_F) + U c_s \frac{dc_s}{dT} + \frac{dE_F}{dT} f_2(E_F) \\ + \frac{(\pi k_B)^2}{3} \left(\rho(e_F) + e_F \frac{d\rho}{d\epsilon}(e_F) + \rho(E_F) + E_F \frac{d\rho}{d\epsilon}(E_F)\right) T \end{array} ,$$

with $f_1(\epsilon) = \epsilon\rho(\epsilon)$, $f_2(\epsilon) = f_1(\epsilon) + \frac{(\pi k_B T)^2}{6} \frac{d^2 f_1}{d\epsilon^2}(\epsilon)$. Due to $\frac{dE_F}{dT} \approx 0 \Rightarrow \frac{dc_s}{dT} \approx 0$, there is $C \propto T$ as for a Fermi gas[1], albeit with $\rho(e_F) + e_F \frac{d\rho}{d\epsilon}(e_F) + \rho(E_F) + E_F \frac{d\rho}{d\epsilon}(E_F)$ instead of $\rho(E_F)$. However whenever e_F happens to be close to ϵ_d, it entails that $\frac{d\rho}{d\epsilon}(e_F)$ diverges like $(e_F - \epsilon_d)^{-.5}$, as expected for a three-dimensional Van Hove singularity, which would increase significantly $\frac{dC}{dT}$.

Whenever an external magnetic field H is applied onto the electrons, the dispersion relations read

$$\epsilon_{t,\pm}(k) = \epsilon(k) \mp \frac{\mu_e H}{2} \quad , \quad (11)$$

with μ_e standing for the electron magnetic moment. Because of $c_{s,+} = c_{s,-} = \frac{c_s}{2}$, as shown above, *only triplet* electrons contribute to the magnetisation per site, expressed thus as

$$M = \mu_e \left(c_{t,+} - c_{t,-}\right) \quad .$$

The corresponding magnetic susceptibility $\chi = \frac{M}{H}(H \to 0)$ reads thence

$$\frac{\chi}{\mu_e^2} = \frac{c_{t,+} - c_{t,-}}{\mu_e H} = -\int_{\epsilon_d}^{\epsilon_u} \rho(\epsilon) \frac{\partial n}{\partial \epsilon}(\epsilon) d\epsilon = a(E_F) \quad .$$

There is $\frac{d\chi}{dT}(T = 0) = 0$ as for a Fermi gas[1]. However, all of *singlet* and *triplet* electrons contribute to the specific heat, whereas only *triplet* ones can contribute to the susceptibility.

V. CONCLUSION

The $\Delta = 0$, $\Delta \neq 0$ solutions of Eqs.(3) have been shown to account for the properties of normal and superconducting[15,17] metals, respectively. The motion of conduction electrons in normal metals, coupled by a strong Coulomb repulsion, is described by Eqs.(4) within the framework of the correlated Fermi gas. Each independent-electron band splits into two one-electron bands, populated by electrons at thermal equilibrium according to the Fermi-Dirac statistics. Those two bands result from the outcome of two-electron scattering differing according to whether the incoming electrons have same or opposite spin direction. Good agreement with Bethe's wave-function data[22,23] has been obtained for the $d = 1$ Hubbard model. The groundstate energy, obtained for the $d = 2$ Hubbard Hamiltonian, turns out to be *lower* than those reckoned with help of numerical schemes[8,25], which makes questionable the claim that they are converged to the groundstate energy for $N \to \infty$. This analysis can be extended to all practical temperatures, including low temperatures which are out of the reach of numerical methods[8]. This work gives also *unique* access to correlation functions, which has enabled us to show that the Hubbard Hamiltonian sustains no kind of long range order for $d = 1, 2, 3$ and any $U > 0, c_0 < 1$ value. At last, contrary to what has been argued elsewhere[7,31,32], the conduction electrons do not go antiferromagnetic for $\frac{U}{t} \to \infty$, since the groundstate energy of the correlated Fermi gas has been shown to be < 0 for $c_0 < 1$, that is *lower* than that of the antiferromagnetic state $= 0$.

The main significance of the correlated Fermi gas is to validate Drude's model[1], as far as the *continuum* states are concerned. Accordingly, the inter-electron coupling turns out to be instrumental *only* at each two-particle scattering event with the Coulomb repulsion with all other electrons playing *no* role. Hence such a picture is seen to be in marked contrast with classical mechanics and the mean-field approach in quantum mechanics for

which *all* of the inter-electron forces are conversely assumed to be *permanently* at work. Finally, the physical meaning of Eqs.(4) is to unveil the reason why conduction electrons behave like *independent* particles in normal metals, despite the *strong* Coulomb repulsion.

VI. APPENDIX

Let us first introduce $h_K^\zeta = \sum_{\zeta',K'} H_{K'}^{\zeta'} - H_K^\zeta$. Then $\left[H_K^\zeta, h_K^\zeta\right] \neq 0$ implies $h_K^\zeta \psi_K^\zeta \in S_2$. Hence taking $\phi_K^\zeta = h_K^\zeta \psi_K^\zeta$ entails

$$H\psi = \left(H_d + H_K^\zeta + h_K^\zeta\right)\left(1 + h_K^\zeta\right)\psi_K^\zeta \quad .$$

The projection φ of $H\psi$ onto S_K^ζ reads

$$\varphi = \left(H_d + H_K^\zeta\right)\psi_K^\zeta + \varphi_2 \quad ,$$

with φ_2 being the projection of $\left(h_K^\zeta\right)^2 \psi_K^\zeta$ onto S_K^ζ. The proof consists of showing $\varphi_2 = 0$ for $N \to \infty$. To that end, it will be taken advantage of ϕ (any vector of the basis of S_K^ζ) and $h_K^\zeta \phi$ differing only by two pairs from each other. For simplicity and without loss of generality, we consider the Hubbard case. Thus let us take

$$\phi = b_{s,K,k_1}^+ b_{s,K,k_2}^+ \, |0\rangle \quad .$$

The projection ϕ_p of $\left(h_K^\zeta\right)^2 \phi$ onto S_K^ζ reads

$$\phi_p = \left(\frac{U}{N}\right)^2 \sum_k b_{s,K,k}^+ b_{s,K,k'}^+ \, |0\rangle \quad ,$$

with $k' = k - k_1 + k_2$. It entails

$$\langle \phi_p \,|\, \phi_p \rangle = \frac{U^4}{N^3} \Rightarrow \varphi_2(N \to \infty) \to 0 \quad ,$$

so that projecting $(H - \varepsilon)\psi = 0$ onto S_K^ζ yields finally

$$(H_d + H_K^\zeta - \varepsilon)\psi_K^\zeta = 0 \quad ,$$

which is the sought conclusion.

ACKNOWLEDGMENTS

The author is beholden to M. Abou Ghantous, F. Beuneu and N. Sandeau for encouragement and to M. Caffarel for checking the consistency of Eqs.(5,6,7) and reckoning the η_g data, plotted in Fig.1.

* corresponding author : jszeftel@lpqm.ens-cachan.fr

[1] N.W. Ashcroft and N. D. Mermin, Solid State Physics, Saunders College (1976)
[2] D.P Arovas *et al.*, arXiv : 2103.12097
[3] L.N. Cooper, Phys. Rev., 104, 1189 (1956)
[4] J. Bardeen, L.N. Cooper and J.R. Schrieffer, Phys.Rev., 108, 1175 (1957)
[5] L.P. Lévy, Magnetism and Superconductivity, Springer (2000)
[6] E. Dagotto, Rev.Mod.Phys., 66, 763 (1994)
[7] J. Spalek, Acta Physica Polonica A, 111, 409 (2007)
[8] J.P.F. LeBlanc *et al.*, Phys.Rev.X, 5, 041041 (2015)
[9] S. Jiang, D.J. Scalapino and S.R. White, *arXiv* : 2104.10149, DOI: 10.1073/pnas.2109978118
[10] W. Kohn and J.M. Luttinger, Phys.Rev.Lett., 15, 524 (1965)
[11] D.J. Scalapino, Rev.Mod.Phys., 84, 1383 (2012)
[12] L. Tocchio, F. Becca and A. Montorsi, Sci.Post.Phys., 6, 018 (2019)
[13] J. Szeftel, N. Sandeau, M. Abou Ghantous and M. El-Saba, J.Supercond.Nov.Magn., 34, 37 (2021)
[14] J. Szeftel, N. Sandeau and M. Abou Ghantous, Eur.Phys.J.B, 92, 67 (2019)
[15] J. Szeftel, N. Sandeau and M. Abou Ghantous, J.Supercond.Nov.Magn., 33, 1307 (2020)
[16] J. Szeftel, N. Sandeau and M. Abou Ghantous, J.Supercond.Nov.Magn. (2021) DOI : 10.1007/s10948-021-06037-z
[17] J. Szeftel, N. Sandeau, M. Abou Ghantous and M. El-Saba, EuroPhys.Lett., 134, 27002 (2021)
[18] J. Szeftel, Acta Physica Polonica A, 85, 329 (1994)
[19] J. Szeftel and A. Khater, Phys.Rev.B, 54, 13581 (1996)
[20] J. Szeftel, in Electron Correlations and Material Properties 2, eds. A. Gonis, N. Kioussis and M. Ciftan, Kluwer Academic, New York (2003)
[21] J. Szeftel and M. Caffarel, J.Phys.A, 37, 623 (2004)
[22] E.H. Lieb and F.Y. Wu, Phys.Rev.Lett., 20, 1445 (1968)
[23] H. Shiba, Phys.Rev.B, 6, 930 (1972)
[24] L. Didukh and Y. Skorenkii, Cond.Matt.Phys., 3, 787 (2000)
[25] E. Dagotto, A. Moreo, F. Ortolani, D. Poilblanc and J. Riera, Phys.Rev.B, 45, 10741 (1992)
[26] L.D. Landau and E.M. Lifshitz, Statistical Physics, Pergamon Press (1959)
[27] J. Szeftel , N. Sandeau and A. Khater, Phys.Lett.A, 381, 1525 (2017)
[28] J. Szeftel , N. Sandeau and A. Khater, Prog.In.Electro.Res.M, 69, 69 (2018)
[29] J. Szeftel, M. Abou Ghantous and N. Sandeau, Prog.In.Electro.Res.L, 81, 1 (2019)
[30] J. Szeftel, N. Sandeau, M. Abou Ghantous and A. Khater, EuroPhys.Lett., 131, 17003 (2020)
[31] N.F. Mott, Rev.Mod.Phys., 40, 677 (1968)
[32] P.W. Anderson, Phys.Rev., 115, 2 (1959)